



Properties and characterization of a metakaolin phosphate acid-based geopolymer synthesized in a humid environment

Teng Dong^{1,2} · Shuibo Xie^{1,2} · Jingsong Wang¹ · Zhenfu Chen¹ · Qing Liu¹

Received: 12 November 2018 / Revised: 19 March 2019 / Accepted: 18 May 2019 / Published online: 1 June 2019
© Australian Ceramic Society 2019

Abstract

To synthesize a metakaolin phosphate acid-based geopolymer (PAG), calcined kaolin and phosphoric acid solutions with phosphorus-to-aluminium molar ratios (P/Al) of 0.6 to 1.0 were prepared. Fresh PAG was cured in a high-humidity environment at 50 °C for 7 days. High humidity is helpful for generating AlPO_4 during the geopolymerization of PAG. Si and Al are depolymerized from metakaolin upon attack of H_3PO_4 , and the amounts of leached Si and Al are directly proportional to P/Al. Leached Al increases with time, while leached Si decreases and then becomes stable. Pyrophosphate and hexa-coordinate Al could be components of the basic structural unit of PAG. Porosity and cracking increased with increasing P/Al and reduced the strength of PAG. The degree of shrinkage and the pore size are directly proportional to P/Al. The concentrated pores in PAG are gel pores, transitional pores and capillary pores corresponding to different P/Al ratios.

Keywords Geopolymer · Metakaolin · Phosphoric acid · Humid environment

Introduction

In recent years, phosphate acid-based geopolymer (PAG) has received considerable attention. Calcined Nanning kaolin [1], calcined raw Tunisia clay [2], Al_2O_3 – 2SiO_2 powders for sol-gel synthesis [3] and other reagents have been employed to synthesize PAG. AlPO_4 was observed in some reports but not in others [2, 4]. The basic structural unit of PAG is uncertain; $-\text{Si}-\text{O}-\text{P}-\text{O}-\text{Si}-$ or $-\text{Si}-\text{O}-\text{Al}-\text{O}-\text{P}-$ has been considered to be the basic unit of the PAG network respectively in different reports [3, 5]. Both tetra-coordinate and hexa-coordinate Al were observed in some reports, while only hexa-coordinate Al was observed in others [1–3]. There are few reports about the depolymerization process of metakaolin under the attack of H_3PO_4 .

In the present study, the humidity of the cured environment was ignored [1–4, 6]. Water evaporated rapidly and gave rise to air bubbles and cracks in PAG when the sample was cured

in an oven at 60 °C [2–4]. A stable temperature and humidity curing conditions are needed to maintain steady, uniform and accelerated geopolymerization. Synthesis of PAG in a high-humidity environment and investigation of the properties and characteristics of PAG are of interest.

The main objective of this work is to investigate the properties and mechanism of PAG synthesis using calcined kaolin (analytical reagent) and phosphoric acid solutions with different P/Al ratios at 50 °C in a wet environment. The amounts of leached Al and Si were determined and used to describe the depolymerization process. The kaolin, calcined kaolin and PAG were characterized using scanning electron microscopy (SEM) coupled to microanalysis by energy-dispersive X-ray analysis (EDX), X-ray diffractometry (XRD), Fourier transform infrared spectroscopy (FTIR) and ^{27}Al , ^{29}Si and ^{31}P magic angle spinning nuclear magnetic resonance (MAS-NMR). The strength, shrinkage and porosity of PAG were determined.

Materials and experimental methods

Kaolin (analytical reagent) was provided by Tianjin Kermel Chemical Reagent Co., Ltd. The chemical composition of kaolin is shown in Table 1. Kaolin mainly consists of SiO_2 (45.35 wt%), Al_2O_3 (39.22 wt%) and Fe_2O_3 (0.31 wt%). Phosphoric acid solutions (H_3PO_4 85%, Hunan Huihong

✉ Shuibo Xie
sbxusc@163.com

¹ School of Civil Engineering, University of South China, Hengyang 421001, Hunan Province, China

² School of Resource Environment and Safety Engineering, University of South China, Hengyang 421001, Hunan Province, China

Table 1 Chemical composition of kaolin

Composition	SiO ₂	Al ₂ O ₃	Fe ₂ O ₃	CaO	MgO	TiO	Loi
Wt%	45.35	39.22	0.31	0.16	0.18	0.22	14.49

Chemical Reagent Co., Ltd) were used to prepare activators with different molar concentrations corresponding to P/Al = 0.6, 0.8 and 1.0. Distilled water was used as a solvent, and the doses of water were fixed. To study the components of PAG, samples were cured at 50 °C at a humidity greater than 98%, while control samples were cured at 50 °C at a humidity lower than 3%. Table 2 and Table 3 show the formulations of PAG samples. Samples MPC, MPD and MPE were cured in a wet environment, and samples SPC, SPD and SPE were cured in a dry environment.

Kaolin was thermally treated in a muffle furnace by first being heated from ambient temperature to 800 °C and then being kept at the selected temperature for 4 h. The obtained specimen was quenched by air at ambient temperature and was stored in a dry environment. Calcined kaolin was mixed with a series of phosphoric acid solutions and stirred in a planetary mortar mixer for 15 min (the mixing pot and mixing blade were made of 304 stainless steel) at room temperature. Fresh PAG was poured into Ø50 mm × 50 mm and 25 mm × 25 mm × 250 mm polypropylene (PP) plastic moulds. The samples were vibrated on a vibrating table for 3 min and then cured for 7 days.

The amounts of leached Si and Al in the fresh geopolymers MPC, MPD and MPE were evaluated. Fresh PAG (0.5 g) was extracted at 1, 3, 6, 9 and 12 h, and distilled water was added to 25 g. The diluted fresh PAG solutions were centrifuged for 30 min at 10,000 rad/min, and the supernatant liquids were analysed. The sampled leachates were analysed by silicon molybdenum blue and chrome azurol S spectrophotometry to evaluate the leached amounts of Si and Al, respectively.

The shrinkage of the 25 mm × 25 mm × 250 mm hardened PAG samples was determined by measuring the expansion rate

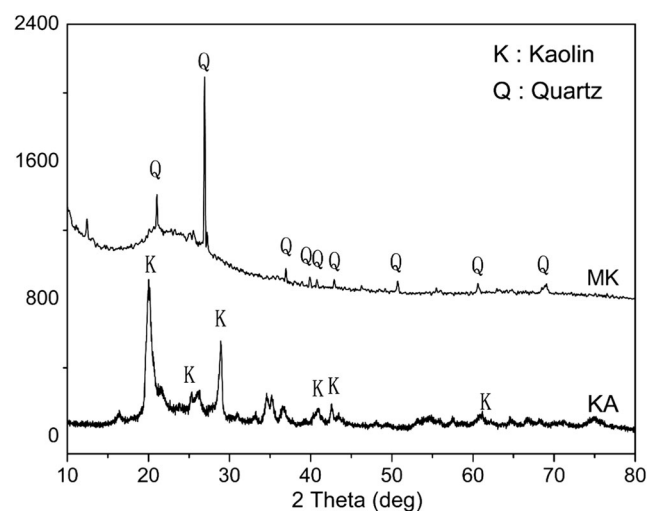
Table 2 Formulations of geopolymers cured in a wet environment at 50 °C

Samples	MPA	MPB	MPC	MPD	MPE	MPF
Water–binder ratio	0.3	0.3	0.3	0.3	0.3	0.3
P/Al	0.2	0.4	0.6	0.8	1.0	1.2

Table 3 Formulations of control groups cured in a dry environment at 50 °C

Samples	SPC	SPD	SPE
Water–binder ratio	0.3	0.3	0.3
P/Al	0.6	0.8	1.0

of shrinkage-compensating concrete. The mechanical properties of the geopolymers were evaluated by measuring the compressive strength. Six Ø50 mm × 50 mm samples were tested to determine each P/Al ratio. The fragments of every sample were collected after the compressive strength test. Pieces of samples MPC, MPD and MPE were collected to prepare the test samples for the mercury intrusion porosimetry (MIP) experiments. An MIP instrument (Autopore IV 9500, Micromeritics) was used to measure the pore size distributions. Porosity was evaluated by using the set time equilibrium (10 s) mode between the pressure limits of 0.69 kPa and 413.40 MPa. Under these operative conditions, MIP can measure the capillary pore range from 0.003 to 1000 µm. Other fragments were milled into powders. Fifty grams of powders was kept in an oven at 105 °C for 12 h, and the powders were again weighed to get the free water of PAG. The powders were used for XRD measurements, FTIR and MAS-NMR experiments. XRD was conducted by using a Bruker D8 ADVANCE instrument under the following conditions: 40 kV, 40 mA and Cu K α radiation. The range of the scanning angle 2θ was between 5 and 80°. FTIR experiments were performed by using a VECTOR33 FTIR spectrometer. The samples were mixed with KBr, and the wavelength was varied from 400 to 4000 cm⁻¹. ²⁷Al, ²⁹Si and ³¹P MAS-NMR experiments were performed by using a Bruker AVANCE III 600 spectrometer.

**Fig. 1** XRD patterns of kaolin (KA) and calcined kaolin (MK)

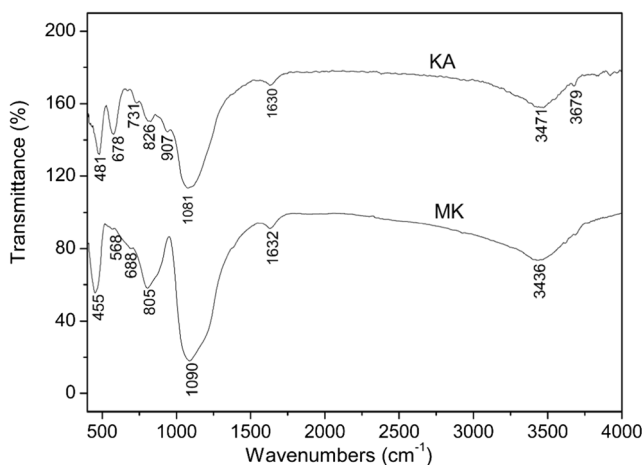


Fig. 2 FTIR spectra of kaolin (KA) and calcined kaolin (MK)

Results and discussion

Characterization of kaolin and calcined kaolin

A comparison between the X-ray patterns of the investigated kaolin (KA) before and after calcination shows that all diffraction peaks corresponding to kaolinite disappeared after heat treatment and a diffuse reflection appeared between 15 and 30° (2θ) (Fig. 1), which proves the transformation of kaolin

into metakaolin [7]. Diffraction peaks corresponding to quartz were observed in calcined kaolin (MK).

The infrared spectra of kaolin and calcined kaolin are shown in Fig. 2. The bands at 907 cm^{-1} ascribed to Al(VI)–OH disappeared, which means that –OH desorbed during the heating process. The band at 826 cm^{-1} , which was ascribed to –Si–O–Al(IV), shifted to 805 cm^{-1} . The bands at 731 cm^{-1} and 678 cm^{-1} disappeared, and the new bands at 688 cm^{-1} were attributed to the –Si–O–Al(V) [8] of metakaolin that appeared in calcined kaolin. Another new band at 568 cm^{-1} , assigned to –Si–O–Al(VI), also appeared in calcined kaolin. The peaks at 1090 cm^{-1} and 455 cm^{-1} were assigned to the stretching and deformation vibrations of Si–O, respectively.

Examination of the ^{29}Si NMR spectra of kaolin (Fig. 3a) shows that there is only one singlet peak at $\delta = -92.7$ ppm. This signal is characteristic of tetrahedral silicon bonded through oxygen to four other silicon atoms (SiQ^3) in a clay mineral [9]. We observed the peak at $\delta = -92.7$ ppm shift to a narrow peak at $\delta = -100.2$ ppm after calcination (Fig. 3a, b). The chemical shift of the spectral peak shows that the degree of polymerization of silicon atoms is still Q3 and that calcined kaolin is still a layered structure. The chemical shift is caused by the change in the bond lengths and bond angles in the structure layer. The peak attributed to calcined kaolin is asymmetrical and is caused by the appearance of quartz. The

Fig. 3 ^{29}Si and ^{27}Al MAS-NMR spectra of kaolin (a, c) and calcined kaolin (b, d)

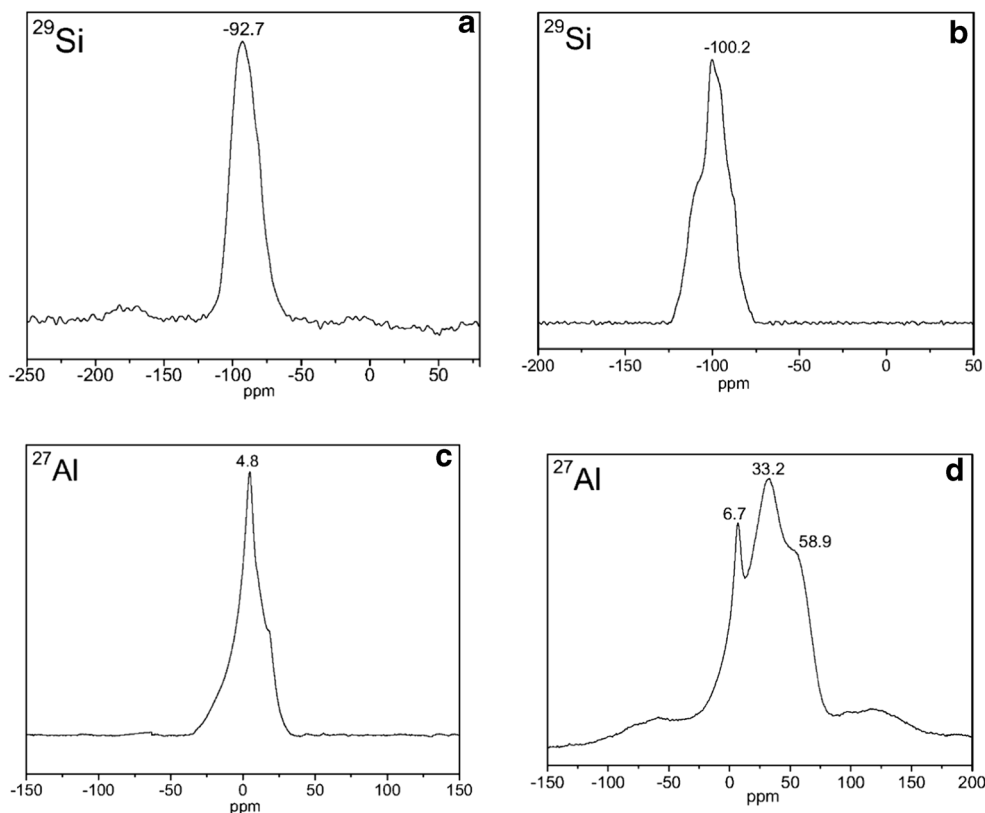
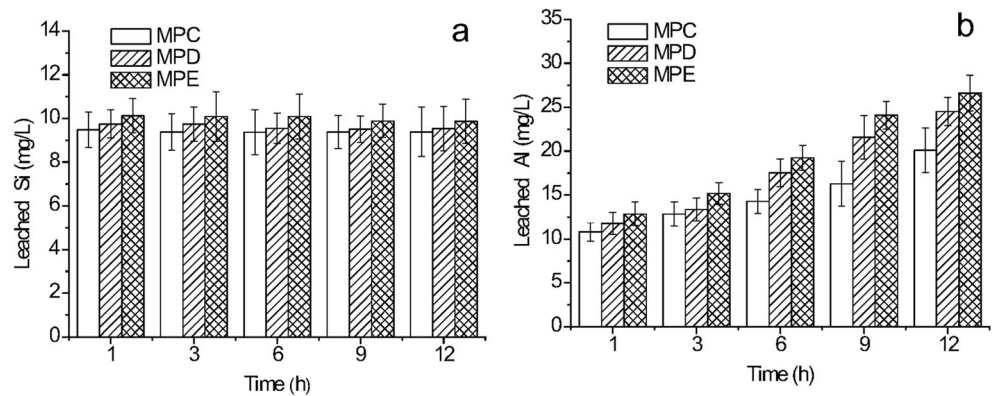


Fig. 4 Leached Si (a) and Al (b) of geopolymers MPC, MPD and MPE



structure of the [SiO₄] tetrahedron changed, and this change could be related to the appearance of quartz during the calcination process [10].

Only one singlet peak at $\delta = 4.8$ ppm was observed in the ²⁷Al NMR spectra of kaolin (Fig. 3c), thus implying that only hexa-coordinate Al is present in kaolin. After calcination at 800 °C for 4 h, the ²⁷Al NMR spectra (Fig. 3d) revealed the presence of peaks at $\delta = 58.9$ ppm and $\delta = 33.2$ ppm assigned to tetra-coordinate and penta-coordinate Al, respectively. The intensity of the peak assigned to penta-coordinate Al is the highest. Hexa-coordinate Al, which gives rise to the peak at $\delta = 6.7$ ppm, is present in calcined kaolin.

Leaching test of Si and Al

Figure 4a shows the amounts of leached Si in samples MPC, MPD and MPE within 12 h. Quartz is insoluble in phosphoric acid at 50 °C, so Si in solution might be oligomeric Si

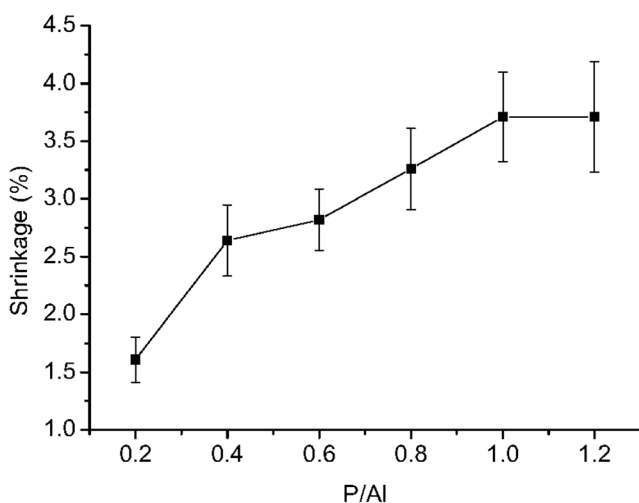


Fig. 5 Shrinkages of geopolymers MPA, MPB, MPC, MPD, MPE and MPF

dissolved from metakaolin. Initially, the amount of leached Si in geopolymers MPC, MPD and MPE was 9.48 mg/L, 9.75 mg/L and 10.13 mg/L, respectively. The amount of leached Si is related to the amount of H⁺; for geopolymers MPC and MPD, the amount of H⁺ may be insufficient, making it difficult for Si to continue dissolving. The amount of leached Si in geopolymer MPE is the highest, which means that most oligomeric Si is available for the polymerization process. There are decreases in the amount of leached Si at 3 h, 6 h and 9 h in MPC, MPD and MPE, respectively, and then the amount becomes stable. This decrease indicates that oligomeric Si dissolved from metakaolin and was then consumed in the polymerization process. Depolymerization is assumed to dominate initially and then polymerization dominates. The stability of the amount of leached Si was mainly due to the PAG gel formed on the surface of undissolved metakaolin particles. This result could explain the slow rate of the reaction.

The O–Al bond of the –Si–O–Al– structure is broken by H⁺, and then Al³⁺ is dissolved. H₂PO₄⁻ and Al³⁺ coexist, and Al accumulates in solution (Fig. 4b). Therefore, leached Al increases with time for 12 h. At the same time, the amount of leached Al also increases with the increase in P/Al ratio.

Mechanical properties and microstructures of PAG

After being cured in a wet environment at 50 °C for 7 days, fresh PAG formed hardened geopolymers. Shrinkage was observed, as shown in Fig. 5, and this shrinkage increased as the P/Al ratio increased; the maximum shrinkage was 3.71% for samples MPE and MPF. Water barely evaporated when the humidity was $\geq 98\%$, and the shrinkage was considered to be chemical shrinkage. Higher P/Al ratios lead to larger chemical shrinkage that causes cracks. As shown in Fig. 6, more cracks were observed in MPE than in MPC and MPD. Small air bubbles were observed (Fig. 6) in the PAG samples that were

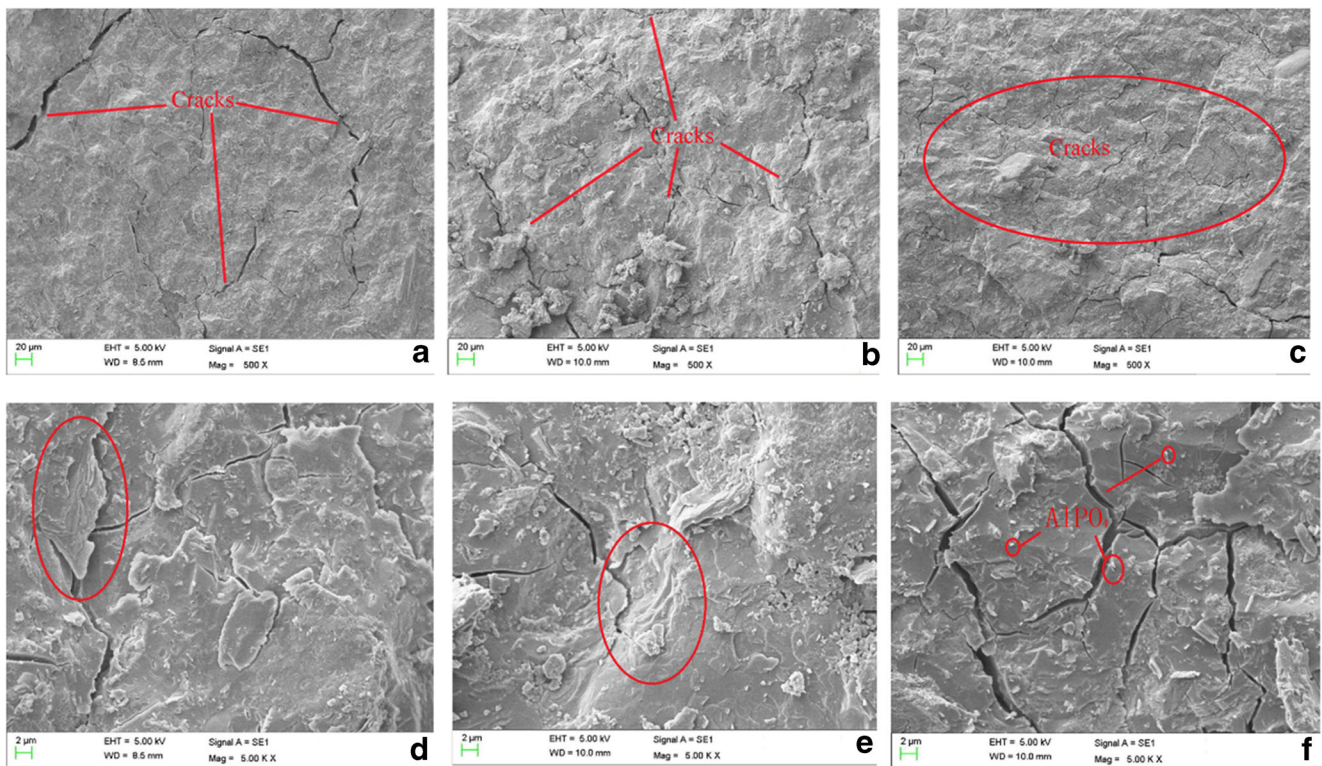


Fig. 6 SEM images of geopolymers MPC (a, d), MPD (b, e), and MPE (c, f)

cured in a humid environment. This finding indicates that the reaction is more steady and uniform in a humid environment.

In the micrograph with a magnification of $\times 5000$ (Fig. 6), layered structures are still observed in samples MPC, MPD and MPE, while the SEM images of MPC, MPD and MPE show the presence of some white points. These white points disappeared in sample SPE

(Fig. 7a, b). The X-ray patterns of PAG are shown in Fig. 8a, b. The diffraction peaks assigned to AlPO_4 were observed in samples MPC, MPD and MPE, while the characteristic peaks disappeared in samples SPC, SPD and SPE. The diffraction peaks of AlPO_4 become increasingly obvious with increasing P/Al (Fig. 7a). The microanalysis of the selected area of sample MPE is

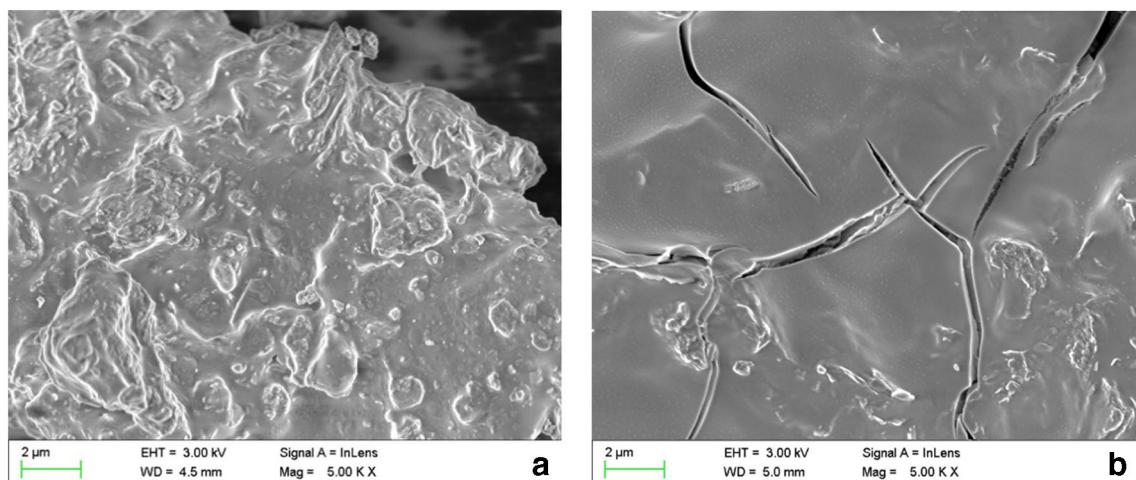
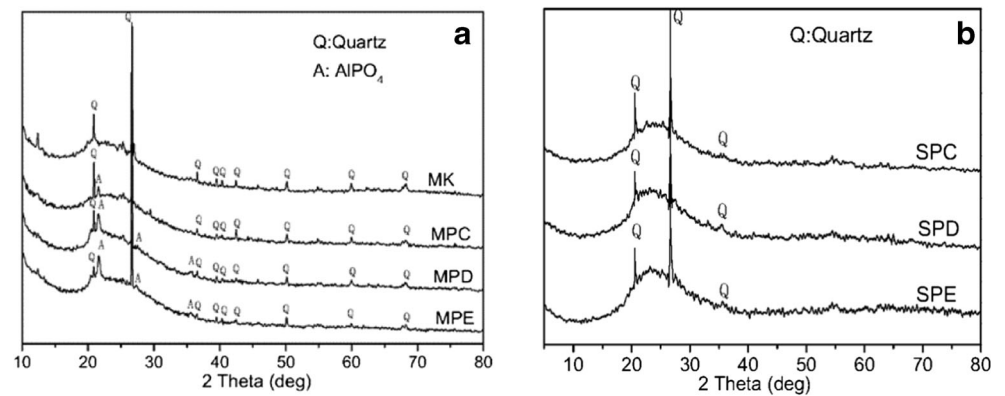


Fig. 7 SEM images of geopolymers MPE (a) and SPE (b)

Fig. 8 XRD patterns of PAG cured in wet and dry environment at 50 °C (**a** wet environment, **b** dry environment)



given in Fig. 9. In zone 01, the Al atom percent is 6.98%, the Si atom percent is 17.79% and the P atom percent is 7.89%. In zone 02, the Al atom percent is 11.56%, the Si atom percent is 2.73% and the P atom percent is 15.74%. The Al and P atom percents in zone 02 are closely related to AlPO_4 . Based on these characteristics, we speculate that the white points in the SEM images are AlPO_4 .

Some reports claim that AlPO_4 acts as a filler to reinforce the structure and increase the compressive strength of PAG. In

these reports, the porosities and cracks of hardened PAG were ignored. In Fig. 10, the amount of free water in samples MPC, MPD and MPE increased from 7.24 to 11.37 g, and the porosities increased from 6.9 to 21.9%. Figure 11 shows that MPC has the highest compressive strength of 117.7 MPa, the lowest porosity (Fig. 10) and fewest cracks (Fig. 6). This result indicated that cracks and pores reduced the compressive strength of PAG. The dose of H_3PO_4 was not sufficient for the reaction in samples MPA and MPB, so the strengths of these samples are lower than that of MPC.

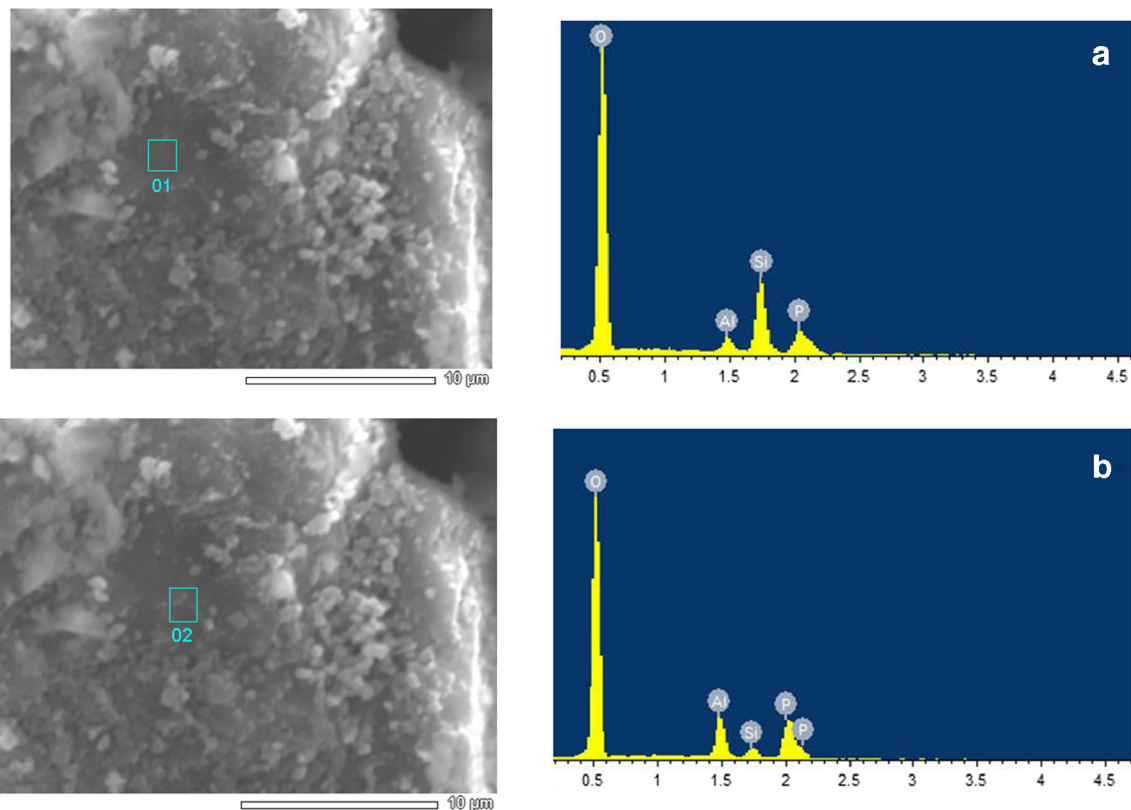


Fig. 9 SEM-EDX analysis of geopolymer MPE (a: analysis of zone01, b: analysis of zone02)

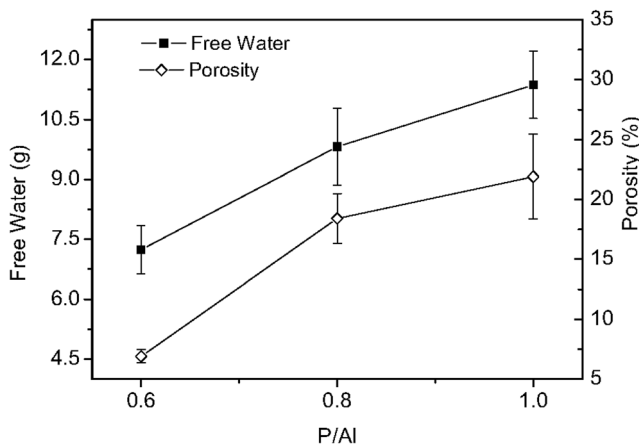


Fig. 10 Free water and porosity of geopolymers MPC, MPD and MPE

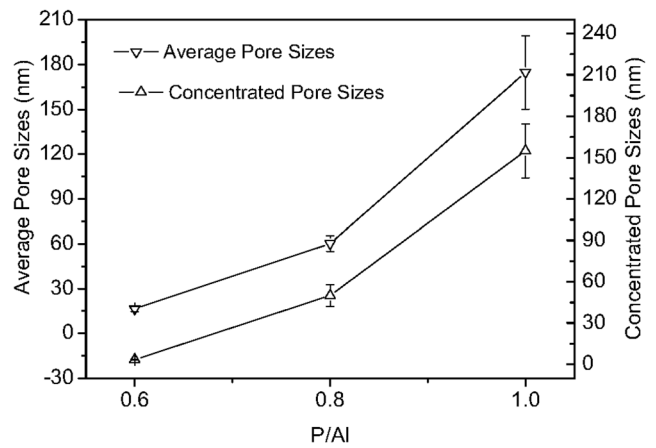


Fig. 12 Average pore sizes and concentrated pore sizes of geopolymers MPC, MPD and MPE

As shown in Fig. 12, the average pore size increased from 16.4 to 174.7 nm, and the concentrated pore sizes increased from 3.5 to 155.2 nm with increasing P/Al. As the porosities increased, the pore size of the PAG increased. The average pore sizes are larger than the concentrated pore sizes (Fig. 12). In Fig. 13a–c, the area occupied by pores constitutes a proportion of the total area, and the diameters of the pores increased with increasing P/Al. No obvious pores were observed in sample MPC at a high magnification of $\times 50,000$ (Fig. 13a) because the concentrated pore size was too small and the pores could be gel pores that exist in the reaction products. The concentrated pores are approximately 50 nm in sample MPD (Fig. 13b); these pores could be transitional pores that exist in between reaction products. The concentrated pore size is approximately 150 nm in sample MPE, and these pores could be capillary pores that formed in the spaces

not occupied by reaction products (Fig. 13c). Free water was generated during geopolymerization, and there could be some capillary pores in all samples; these capillary pores make the average pore size larger than the concentrated pore size.

Geopolymer characterization

In Fig. 8a, b, some diffraction peaks correspond to quartz in MK, wet cured samples and dry cured samples. It appears that the quartz remains unaffected during the geopolymerization process. The samples exhibit an amorphous characteristic in the XRD patterns for 2θ in the $20\text{--}30^\circ$ range (Fig. 8a, b), which indicates that the structure of the PAG is typically glass-like.

The FTIR spectra of PAG with different P/Al ratios are presented in Fig. 14. In agreement with the XRD results, the FTIR spectra show the disappearance of the metakaolin bands and the appearance of new bands that are related to a new species. The wavenumbers of the principal FTIR bands and their corresponding species are listed below:

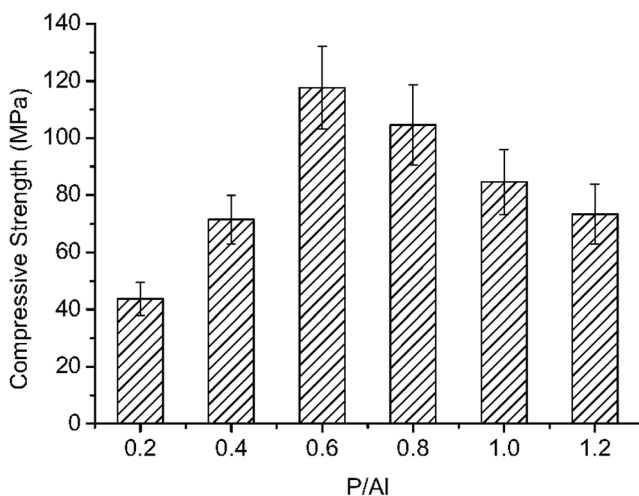


Fig. 11 Strengths of geopolymers MPC, MPD and MPE

- i. The bands at 1645 cm^{-1} and 3422 cm^{-1} correspond to the stretching and deformation vibrations of the O–H and H–O–H groups in the water molecules in the hardened PAG, respectively [11].
- ii. The peak attributed to Si–O symmetrical vibration of metakaolin at 1090 cm^{-1} shifts by approximately 5 to 1095 cm^{-1} after the geopolymerization reaction. For MPE, new bands at 796 cm^{-1} could be related to $-\text{Si}-\text{O}-\text{P}-$ [12]. The metakaolin bands at 455 cm^{-1} ascribed to the $-\text{Si}-\text{O}-\text{Si}-$ shift to 467 cm^{-1} in the hardened PAG. This shift indicates that the Si–O changed to $-\text{Si}-\text{O}-\text{P}-$ [2], which may be attributed to the partial replacement of

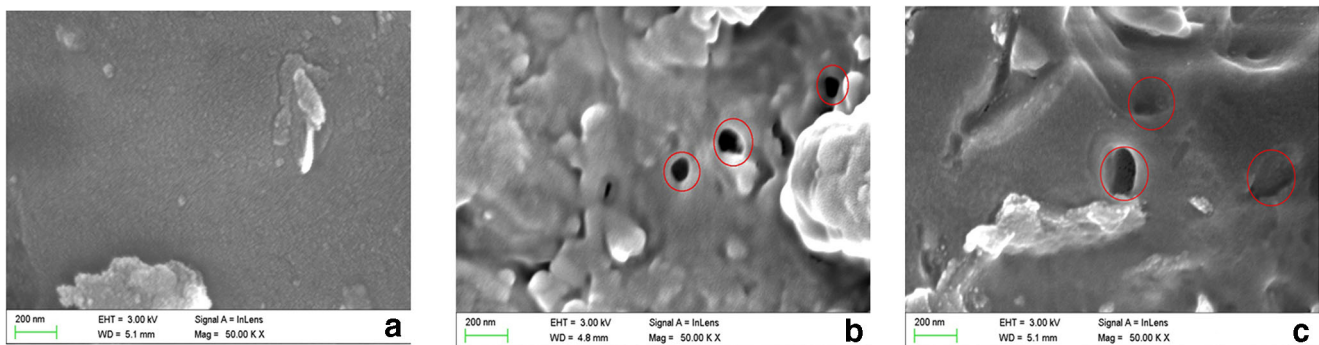


Fig. 13 Concentrated pores of geopolymers MPC (a), MPD (b) and MPE (c)

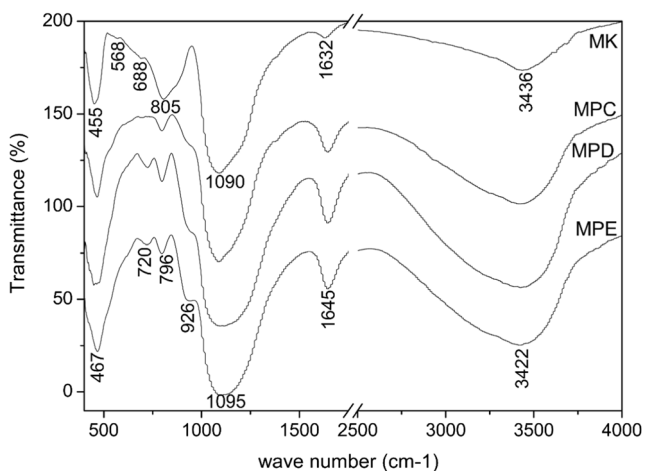


Fig. 14 FTIR spectra of geopolymers MPC, MPD and MPE

the [SiO₄] tetrahedron by a [PO₄] tetrahedron, resulting in a change in the local chemical environment. This structural change occurs during the geopolymerization reaction and leads to the formation of new products with a microstructure different from that of metakaolin. This finding implies the formation of $-\text{Si}-\text{O}-\text{P}-\text{O}-\text{Si}-$ in the geopolymer network [4].

- iii. The bands at 805 cm^{-1} , 688 cm^{-1} and 568 cm^{-1} related to $-\text{Si}-\text{O}-\text{Al}(\text{IV})$, $-\text{Si}-\text{O}-\text{Al}(\text{V})$ and $-\text{Si}-\text{O}-\text{Al}(\text{VI})$, respectively, in metakaolin disappear after geopolymerization. New bands at 720 cm^{-1} are observed in MPC, MPD and MPE. The intensity of this band increases with increasing P/Al. This band could indicate the formation of $-\text{P}-\text{O}-\text{Al}-$.
- iv. The bands at 926 cm^{-1} are attributed to $-\text{P}-\text{O}-\text{P}-$ vibrations [13].

In the ^{29}Si MAS-NMR spectra of samples MPC, MPD and MPE (Fig. 15a), three chemical shifts at $\delta = -90.4\text{ ppm}$, $\delta = -101.3\text{ ppm}$ and $\delta = -110.5\text{ ppm}$ correlated to the Q3, Q4 (mAl, nP) and Q4 environments are observed. The lowest-intensity resonance ($\delta = -90.4\text{ ppm}$) represents the rearrangement of some kaolin structure segments. The $\delta = -90.4\text{ ppm}$ resonance is a characteristic feature of the Q3 environment, whereas the $\delta = -101.3\text{ ppm}$ resonance describes the mixed Q4 (mAl, nP) environment species resulting from the polymerization [14]. The strongest resonance at $\delta = -110.5\text{ ppm}$ is attributed to the existing siliceous structures due to the Al-free portions of the original metakaolin structure. Al was depolymerized from metakaolin under the attack of H_3PO_4 , and the dealuminated Si layers were retained in PAG; this Si

Fig. 15 ^{29}Si MAS-NMR spectra of geopolymers cured in wet and dry environment at $50\text{ }^\circ\text{C}$ (a wet environment, b dry environment)

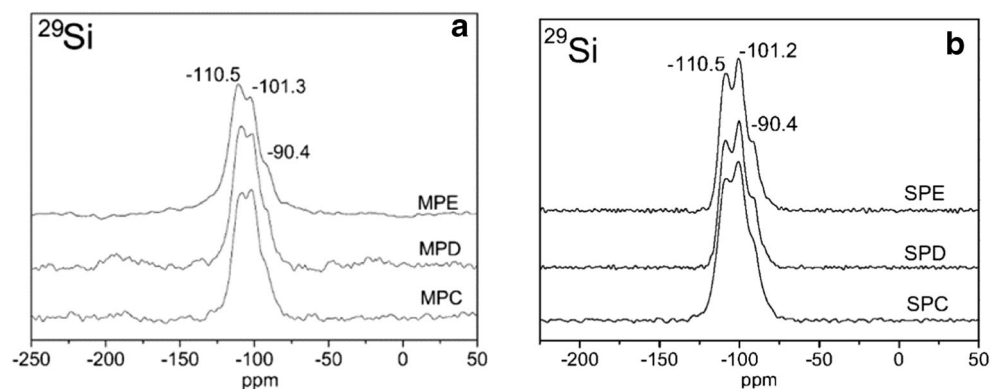
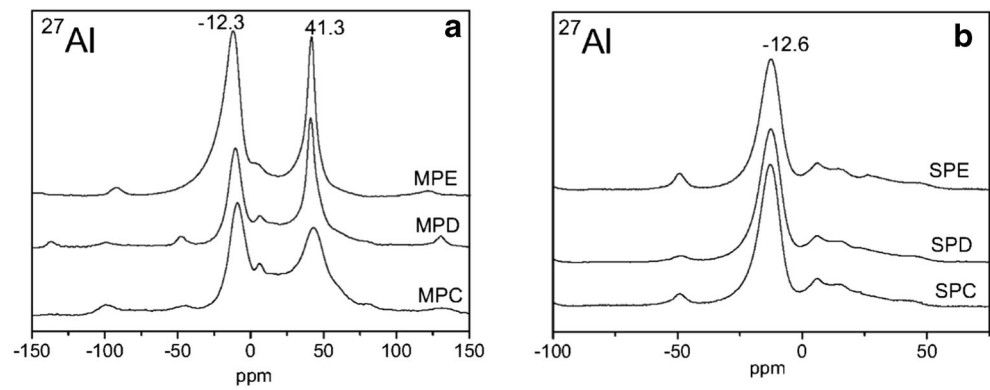


Fig. 16 ^{27}Al MAS-NMR spectra of geopolymers cured in wet and dry environment at 50 °C (**a** wet environment, **b** dry environment)



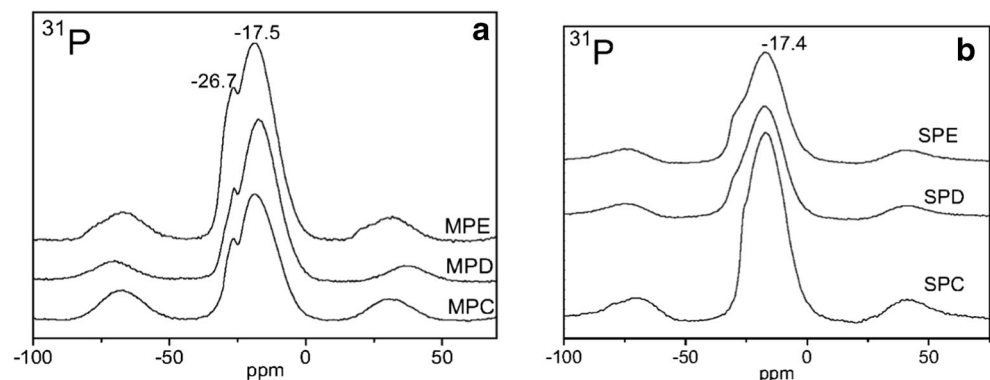
gives rise to the $\delta = -110.5$ ppm resonance. Oligomerized Si depolymerizes from metakaolin under the attack of H_3PO_4 , and this oligomerized Si reacted with $[\text{AlO}_4]$ tetrahedron and $[\text{PO}_4]$ tetrahedron gives rise to the $\delta = -101.3$ ppm resonance. The ^{29}Si spectra of samples SPC, SPD and SPE are most similar to that of samples cured in a wet environment (Fig. 15b).

For MPC, MPD and MPE, the $\delta = 58.9$ ppm, $\delta = 33.2$ ppm and $\delta = 6.7$ ppm resonances in the ^{27}Al MAS-NMR spectra of metakaolin are tetra-coordinate aluminium, penta-coordinate aluminium and hexa-coordinate aluminium (Fig. 16a). These resonances correspond to the peaks at 805 cm^{-1} , 688 cm^{-1} and 568 cm^{-1} in the FTIR spectra, representing $-\text{Si}-\text{O}-\text{Al}(\text{IV})$, $-\text{Si}-\text{O}-\text{Al}(\text{V})$ and $-\text{Si}-\text{O}-\text{Al}(\text{VI})$, respectively. In the geopolymers, the penta-coordinate aluminium completely disappeared, and tetra-coordinate aluminium with $\delta = 41.3$ ppm and hexa-coordinate aluminium with $\delta = -10.6$ ppm were observed in samples MPC, MPD and MPE (Fig. 16a). Since $-\text{Si}-\text{O}-\text{Al}-$ disappeared, the two kinds of aluminium present are assigned to the aluminium in the products of geopolymerization. For dry cured samples SPC, SPD and SPE, the tetra-coordinate aluminium disappeared, and

only hexa-coordinate aluminium was observed in the ^{27}Al MAS-NMR spectra (Fig. 16b). With the increase in P/Al, the characteristic peaks of tetra-coordinate aluminium became increasingly obvious (Fig. 16a), which is consistent with the characteristic peaks of the AlPO_4 diffraction pattern. The tetra-coordinate aluminium observed could be AlPO_4 . Al depolymerized from metakaolin exists in PAG network in the form of hexa-coordinate aluminium.

Figure 17a and b show the ^{31}P MAS-NMR spectra of the samples. For samples MPC, MPD and MPE, a resonance at $\delta = -26.5$ ppm (Fig. 8) was observed, while these peaks disappeared in samples SPC, SPD and SPE. The $\delta = -26.5$ ppm resonance could be the characteristic peak of AlPO_4 [15]. A $\delta = -17.5$ ppm resonance was observed (Fig. 17a, b) in all samples, and these peaks indicate amorphous P of PAG [16]. $-\text{P}-\text{O}-\text{P}-$ vibrations were observed in the FTIR spectra of PAG (Fig. 14). The $\delta = -17.5$ ppm resonance is the characteristic shift of pyrophosphate. The heat released from geopolymerization accumulates in the reaction, and PO_4^{3-} polycondenses to pyrophosphate. We speculate that PO_4^{3-} polymerized into pyrophosphate and that pyrophosphate could be a component of the basic structural unit of PAG.

Fig. 17 ^{31}P MAS-NMR spectra of geopolymers cured in wet and dry environment at 50 °C (**a** wet environment, **b** dry environment)



Conclusion

The main findings of this study can be summarized as follows:

When metakaolin is mixed with phosphoric acid solution, the amount of leached Al increases over time, while the amount of leached Si decreases and then tends to be stable. The amounts of leached Al and Si are directly proportional to the P/Al ratio.

High humidity is helpful for generating AlPO_4 during geopolymerization of PAG. Pyrophosphate and tetra-coordinate Al are considered the components of the basic structural unit of PAG.

The maximum compressive strength of PAG was 117.7 MPa when P/Al is equal to 0.6. As P/Al increased, the free water, porosity and cracking increased. The presence of pores and cracks reduced the strength of PAG. The degree of shrinkage and the average pore size are directly proportional to P/Al. The concentrated pores are gel pores, transitional pores and capillary pores in PAG corresponding to different P/Al ratios.

Funding information The authors gratefully acknowledge the Research Foundation of Education Bureau of Hunan Province, China (Grant No. 18K075) and the National Natural Science Foundation of China (Grant No. 51678286).

References

- Cao, D., Su, D., Lu, B., Yang, Y.: Synthesis and structure characterization of geopolymeric material based on metakaolinite and phosphoric acid. *J. Chin. Ceram. Soc.* **33**, 1385–1389 (2005)
- Louati, S., Hajjaji, W., Baklouti, S., Samet, B.: Structure and properties of new ecomaterial obtained by a phosphoric acid attack of natural Tunisian clay. *Appl. Clay Sci.* **101**, 60–67 (2014)
- Liu, L.P., Cui, X.M., He, Y., Liu, S.D., Gong, S.Y.: The phase evolution of phosphoric acid-based geopolymers at elevated temperatures. *Mater. Lett.* **66**(1), 10–12 (2012)
- Tchakouté, H.K., Rüscher, C.H.: Mechanical and microstructural properties of metakaolin-based geopolymer cements from sodium waterglass and phosphoric acid solution as hardeners: a comparative study. *Appl. Clay Sci.* **140**, 81–87 (2017)
- Davidovits, J.: *Geopolymer Chemistry and Applications*. 1st ed, PP: 196, National defense industry press, Beijing (2011)
- Tchakouté, H.K., Rüscher, C.H., Kamseu, E., Andreola, F., Leonelli, C.: Influence of the molar concentration of phosphoric acid solution on the properties of metakaolin-phosphate-based geopolymer cements. *Appl. Clay Sci.* **147**, 184–194 (2017)
- Chakchouk, A., Samet, B., Mnif, T.: Study on the potential use of Tunisian clays as pozzolanic material. *Appl. Clay Sci.* **33**(2), 79–88 (2006)
- Li, G., Ai, L., Jiang, T., et al.: Structural transformation and acid dissociation behaviors of aluminum from kaolinite under thermal activation. *J. Chin. Ceram. Soc.* **36**(9), 1200–1204+1219 (2008)
- Engelhard, G., Michel, D.: *High Resolution Solid-State NMR of Silicates and Zeolites*, p. 184. John Wiley and Sons, New York (1987)
- He, H.P., Hu, C., Guo, J.G., et al.: ^{29}Si and ^{27}Al MAS NMR study of the thermal transformations of kaolinite. *Chin. Sci. Bull.* **38**(6), 570–572 (1993)
- Elimbi, A., Tchakoute, H.K., Njopwouo, D.: Effects of calcinations temperature of kaolinite clays on the properties of geopolymer cements. *Constr. Build. Mater.* **25**, 2805–2812 (2011)
- Stoch, L., Środa, M.: Infrared spectroscopy in the investigation of oxide glasses structure. *J. Mol. Struct.* **511**, 77–84 (1999)
- Yang, N.R., Yue, R.H.: *The Handbook of Inorganic Matalloid Materials Atlas*, 1st edn, p. 213. Wuhan university of technology press, Wuhan (2000)
- Perera, D.S., Hanna, J.V., Davis, J.: Relative strength of phosphoric acid-reacted and alkali-reacted metakaolin materials. *J. Mater. Sci.* **43**, 6562–6566 (2008)
- Yang, N.R., Yue, R.H.: *The Handbook of Inorganic Matalloid Materials Atlas*, 1st edn, p. 588. Wuhan university of technology press, Wuhan (2000)
- Liu, G.Y., Tian, P., Zhang, Y.: Synthesis of SAPO-34 templated by diethylamine: crystallization process and Si distribution in the crystals. *Microporous Mesoporous Mater.* **114**, 416–423 (2008)

Publisher's note Springer Nature remains neutral with regard to jurisdictional claims in published maps and institutional affiliations.